Loss of *CDC5* Function in *Saccharomyces cerevisiae* Leads to Defects in Swe1p Regulation and Bfa1p/Bub2p-Independent Cytokinesis

Chong Jin Park,* Sukgil Song,* Philip R. Lee,* Wenying Shou,† Raymond J. Deshaies†,‡ and Kyung S. Lee*,[1]

**Laboratory of Metabolism, Center for Cancer Research, National Cancer Institute, National Institutes of Health, Bethesda, Maryland 20892 and †Division of Biology and ‡Howard Hughes Medical Institute, California Institute of Technology, Pasadena, California 91125*

Manuscript received May 31, 2002
Accepted for publication October 9, 2002

ABSTRACT

In many organisms, polo kinases appear to play multiple roles during M-phase progression. To provide new insights into the function of budding yeast polo kinase Cdc5p, we generated novel temperature-sensitive *cdc5* mutants by mutagenizing the C-terminal domain. Here we show that, at a semipermissive temperature, the *cdc5-3* mutant exhibited a synergistic bud elongation and growth defect with loss of *HSL1*, a component important for normal G_2/M transition. Loss of *SWE1*, which phosphorylates and inactivates the budding yeast Cdk1 homolog Cdc28p, suppressed the *cdc5-3 hsl1*Δ defect, suggesting that Cdc5p functions at a point upstream of Swe1p. In addition, the *cdc5-4* and *cdc5-7* mutants exhibited chained cell morphologies with shared cytoplasms between the connected cell bodies, indicating a cytokinetic defect. Close examination of these mutants revealed delayed septin assembly at the incipient bud site and loosely organized septin rings at the mother-bud neck. Components in the mitotic exit network (MEN) play important roles in normal cytokinesis. However, loss of *BFA1* or *BUB2*, negative regulators of the MEN, failed to remedy the cytokinetic defect of these mutants, indicating that Cdc5p promotes cytokinesis independently of Bfa1p and Bub2p. Thus, Cdc5p contributes to the activation of the Swe1p-dependent Cdc28p/Clb pathway, normal septin function, and cytokinesis.

IN various organisms, polo kinases have been shown to regulate diverse cellular and biochemical events at different stages of M phase (for reviews see Lane and Nigg 1997; Glover *et al.* 1998). Data obtained from higher eukaryotic organisms show that, at the G_2/M transition, polo kinase activates cyclin B1-dependent Cdc2 activity through activation of Cdc25C phosphatase (Kumagai and Dunphy 1996) and also through direct phosphorylation and targeting of cyclin B1 to the nucleus (Toyoshima-Morimoto *et al.* 2001). In budding yeast, it is widely appreciated that mitotic entry is tightly linked with proper septin ring organization at the bud neck. A defect in septin assembly causes a Swe1p-dependent G_2 delay, which results in a filamentous phenotype due to the inability of buds to switch from polarized to isotropic growth (Lew and Reed 1993; Barral *et al.* 1999; Edgington *et al.* 1999). A recent report suggests that the polo homolog, Cdc5p, is a potential negative regulator of Swe1p (Bartholomew *et al.* 2001), which inhibits Cdc28 (Cdk1 of budding yeast) by phosphorylating a conserved tyrosine at position 19 (Booher *et al.* 1993). Hsl1p, whose activity depends on proper septin function (Barral *et al.* 1999), acts as a negative regulator of Swe1p (Ma *et al.* 1996). Both Hsl1p and its adaptor Hsl7p are required for the bud-neck localization and degradation of Swe1p (McMillan *et al.* 1999; Shulewitz *et al.* 1999) and thus play a critical role for the Swe1p-dependent Cdc28p activation pathway at the G_2/M transition. During anaphase in mammalian cells or at mitotic exit in budding yeast, polo kinase activates the anaphase-promoting complex (APC; Descombes and Nigg 1998; Shirayama *et al.* 1998), which in turn ubiquitinates the mitotic cyclins, leading to their degradation and the inactivation of Cdk1p. This step is thought to be a prerequisite for the initiation of cytokinesis.

Cytokinesis is a highly coordinated cellular process achieved by contractile ring formation; subsequent contraction of this ring divides one cell into two cells. Temporal and spatial regulation of the cytokinetic machinery is pivotal to ensuring equal partitioning of genomic and cellular materials into two dividing cells. In budding yeast, the future cytokinesis site is specified early in the cell cycle and cleavage is achieved by an actomyosin-based contractile ring, followed by septum formation to separate two dividing cells (Bi *et al.* 1998; Lippincott and Li 1998b). Four septin proteins (Cdc3p, Cdc10p, Cdc11p, and Cdc12p; for review see Longtine *et al.* 1996) are the major structural components of the filaments located at the bud neck (Frazier *et al.* 1998) and form a ring encircling the mother-bud neck. Septin rings appear to play a key role in recruiting much of

[1]*Corresponding author:* Laboratory of Metabolism, National Cancer Institute, NIH, 9000 Rockville Pike, Bldg. 37, Rm. 3D25, Bethesda, MD 20892. E-mail: kyunglee@pop.nci.nih.gov

the cytokinesis machinery to the mother-bud neck. In a septin-dependent manner, Myo1p (myosin II) assembles into a ring at the future budding site early in the cell cycle, whereas F-actin is recruited to the ring just prior to spindle disassembly and contraction (Bi *et al.* 1998; Lippincott and Li 1998a,b). The septin ring disassembles and relocalizes to the future budding site at the time of contraction (Lippincott and Li 1998a). In addition to roles in cytokinesis, septins appear to be critical for diverse cellular functions such as in chitin deposition (DeMarini *et al.* 1997), bud site selection (Chant *et al.* 1995), pheromone-induced morphogenesis (Giot and Konopka 1997), mother-daughter cell compartmentalization (Barral *et al.* 2000; Takizawa *et al.* 2000), and the coordination of mitotic entry with morphogenesis (Carroll *et al.* 1998; Barral *et al.* 1999; Edgington *et al.* 1999; Shulewitz *et al.* 1999; Longtine *et al.* 2000).

A growing body of evidence from various organisms suggests that polo kinases also play important roles in regulating cytokinesis (Ohkura *et al.* 1995; Mundt *et al.* 1997; Bahler *et al.* 1998; Carmena *et al.* 1998; Lee *et al.* 1999; Song and Lee 2001; Tanaka *et al.* 2001). In budding yeast, overexpression of *CDC5* or of its mammalian functional homolog Plk1 leads to the induction of additional septin ring structures (Lee and Erikson, 1997; Lee *et al.* 1999), whereas overexpression of the C-terminal domain of *CDC5* (*cdc5*Δ*N*) induces a dominant-negative cytokinesis defect, likely by disturbing septin structures through a direct interaction between Cdc11p/Cdc12p and cdc5pΔN (Song and Lee 2001). Recent studies have shown that, besides their roles in mitotic exit, components in the mitotic exit network (MEN) such as Cdc5p, Tem1p, Cdc15p, Mob1p, and Cdc14p are required for actin ring formation at the mother-bud neck (Jimenez *et al.* 1998; Frenz *et al.* 2000; Lee *et al.* 2001a). The Tem1p GTPase appears to contribute to actomyosin and septin dynamics during cytokinesis (Lippincott *et al.* 2001). In addition, Bub2p, a putative GTPase activating protein (GAP), has been shown to be important in restraining actin ring formation and cytokinesis (Lee *et al.* 2001b). Bfa1p and Bub2p are closely related to *Schizosaccharomyces pombe* Byr4p and Cdc16p, respectively, which constitute a two-component GAP for the Spg1p GTPase (Furge *et al.* 1998), suggesting that a Bfa1p/Bub2p heteromeric complex negatively regulates Tem1p. Taken together, in addition to their role at mitotic exit, the MEN contributes to cytokinesis and Bfa1p/Bub2p negatively regulates the MEN.

Studies have shown that the C-terminal noncatalytic domain of polo kinases appears to play a critical role in their subcellular localization (Lee *et al.* 1998; Song *et al.* 2000). Overexpression of a kinase-inactive form of *CDC5* under control of the *GAL1* promoter suppresses a *GAL1-SWE1*-induced cell growth defect (Bartholomew *et al.* 2001), whereas overexpression of *cdc5*Δ*N* inhibits cytokinesis (Song and Lee 2001). However, it is unknown whether the C-terminal domain of Cdc5p plays an important role in a Swe1p-dependent pathway or in cytokinesis under physiological conditions. To explore these possibilities, we generated novel temperature-sensitive *cdc5* mutants by randomly mutagenizing the C-terminal domain of Cdc5p. Our data demonstrate that Cdc5p is required for the Swe1p-dependent Cdc28p/Clb activation pathway, normal septin function, and cytokinesis. Multiple mitotic defects observed with C-terminal domain mutants suggest that the C-terminal region of Cdc5p may be a multi-functional domain able to interact with various cellular proteins at different points of M phase.

MATERIALS AND METHODS

Strains, growth conditions, and cell counts: Yeast strains used in this study are shown in Table 1. Cells were cultured in YEP (1% yeast extract, 2% Bacto-peptone) supplemented with 2% glucose. Synthetic minimal medium (Sherman *et al.* 1986) supplemented with the appropriate nutrients was employed to select for plasmid maintenance. Yeast transformation was carried out by the lithium acetate method (Ito *et al.* 1983). All the cells were counted after separating cell aggregates by sonicating with sonicator model W-225R (Heat systems-Ultrasonics, Plainview, NY) at 40% duty with no. 4 output for 4 sec.

PCR mutagenesis of the C-terminal domain of Cdc5: The C-terminal domain of Cdc5p was mutagenized by polymerase chain reaction. To facilitate analyses of various mutants, *CDC5* was C-terminally tagged with three copies of hemagglutinin (HA) epitope tag to generate YCplac22-*CDC5-HA3*. A *Hpa*I/*Pad*I fragment, which includes amino acid residues 366–705, but does not include the HA epitope, was mutagenized as described previously (Muhlrad *et al.* 1992). These PCR products were digested with *Hpa*I and *Pad*I. The fragments obtained were inserted into YCplac22-*CDC5/W517F/V518A/L530A* (Song *et al.* 2000) digested with corresponding enzymes. The resulting *cdc5* mutant library was transformed into the *cdc5*Δ + YCplac33-*CDC5* strain to examine the growth phenotype after shuffling the *URA3*-based *CDC5* plasmid on 5-fluoroorotic acid (5-FOA) plates. All potential temperature-sensitive alleles of *CDC5* were sequenced to determine the mutation sites in the C-terminal domain.

Strain construction: Temperature-sensitive alleles of *CDC5*, which do not support cell viability at 37°, were integrated at the *TRP1* locus of a W303-1A-derived *cdc5*Δ strain (KLY2372) that is kept viable by the presence of a *URA3*-based YCplac33-*CDC5*. After shuffling the YCplac33-*CDC5* plasmid on 5-FOA plates, these mutants were subjected to further analyses. To facilitate analyses of these mutants, *TUB1-GFP* or *CDC10-YFP* (Song *et al.* 2000) was integrated and expressed under the native promoter. To alleviate the mitotic exit defect of *cdc5* mutant strains, a dominant allele of *CDC14* (*CDC14*$^{TAB6\text{-}1}$; Shou *et al.* 2001) was integrated at the *HIS3* locus. Both a *bfa1*Δ*::his5*$^{+}$ and a *bub2*Δ*::his5*$^{+}$ were generated by the one-step gene disruption method described previously (Longtine *et al.* 1998).

Kinase assays and Western analyses: Cell lysates were prepared in TED buffer [40 mm Tris-Cl (pH 7.5), 0.25 mm EDTA, 1 mm dithiothreitol, 1 mm 4-(2-aminoethyl)-benzenesulfonyl fluoride (Pefabloc; Boehringer Mannheim, Indianapolis), 10 μg/ml pepstatin A, 10 μg/ml leupeptin] with an equal volume of glass beads (Sigma, St. Louis). To measure the Cdc5p-HA3-

TABLE 1

Strains used in this study

Strains	Genotype
KLY1546[a]	*MAT***a** *his3-11, 15 leu2-3, 112 trp1-1 ura3*
KLY1548	*MAT*α KLY1546
KLY2372	KLY1546 *cdc5*Δ*::KanMX6 LEU2::TUB1-GFP + YCplac33-CDC5*
KLY2458	KLY1546 *LEU2::TUB1-GFP cdc5*Δ*::KanMX6 TRP1::cdc5-1-HA3*
KLY2460	KLY1546 *LEU2::TUB1-GFP cdc5*Δ*::KanMX6 TRP1::cdc5-3-HA3*
KLY2462	KLY1546 *LEU2::TUB1-GFP cdc5*Δ*::KanMX6 TRP1::cdc5-4-HA3*
KLY2464	KLY1546 *LEU2::TUB1-GFP cdc5*Δ*::KanMX6 TRP1::cdc5-7-HA3*
KLY2470	KLY1546 *LEU2::TUB1-GFP cdc5*Δ*::KanMX6TRP1::CDC5-HA3*
KLY2946	KLY2458 *HIS3::CDC14*$^{TAB6\text{-}1}$
KLY2950	KLY2460 *HIS3::CDC14*$^{TAB6\text{-}1}$
KLY2954	KLY2462 *HIS3::CDC14*$^{TAB6\text{-}1}$
KLY2958	KLY2464 *HIS3::CDC14*$^{TAB6\text{-}1}$
KLY2970	KLY2470 *HIS3::CDC14*$^{TAB6\text{-}1}$
KLY4130	*MAT***a**/α KLY2946/KLY1548
KLY4131	*MAT***a**/α KLY2950/KLY1548
KLY4132	*MAT***a**/α KLY2954/KLY1548
KLY4133	*MAT***a**/α KLY2958/KLY1548
KLY3076	KLY1546 *cdc5*Δ*::KanMX6 TRP1::cdc5-3-HA3 HIS3::CDC14*$^{TAB6\text{-}1}$ *swe1*Δ*::LEU2*
KLY3122	KLY1546 *cdc5*Δ*::KanMX6 TRP1::cdc5-4-HA3 HIS3::CDC14*$^{TAB6\text{-}1}$ *swe1*Δ*::LEU2*
KLY3155	KLY1546 *cdc5*Δ*::KanMX6 TRP1::cdc5-7-HA3 HIS3::CDC14*$^{TAB6\text{-}1}$ *swe1*Δ*::LEU2*
KLY3080	KLY1546 *cdc5*Δ*::KanMX6 TRP1::cdc5-3-HA3 HIS3::CDC14*$^{TAB6\text{-}1}$
KLY2868	KLY1546 *hsl1*Δ*::URA3*
KLY3170	KLY3080 *hsl1*Δ*::URA3*
KLY3173	KLY3080 *hsl1*Δ*::URA3 swe1*Δ*::LEU2*
KLY3071	KLY2954 *URA3::YFP-CDC10*
KLY3072	KLY2958 *URA3::YFP-CDC10*
KLY3075	KLY2970 *URA3::YFP-CDC10*
KLY3205	KLY2462 *URA3::YFP-CDC10*
KLY3206	KLY2464 *URA3::YFP-CDC10*
KLY3209	KLY2470 *URA3::YFP-CDC10*
KLY3578	KLY1546 *cdc5*Δ*::KanMX6 TRP1::cdc5-7-HA3 HIS3::CDC14*$^{TAB6\text{-}1}$ *LEU2::YFP-CDC10*
KLY2374	KLY1546 *bfa1*Δ*::his5*$^{+}$
KLY2573	KLY1546 *bub2*Δ*::his5*$^{+}$
KLY3826	KLY1546 *cdc5*Δ*::KanMX6 URA3::YFP-CDC10 TRP1::cdc5-1-HA3 bfa1*Δ*::his5*$^{+}$
KLY3831	KLY1546 *cdc5*Δ*::KanMX6 URA3::YFP-CDC10 TRP1::cdc5-1-HA3 bub2*Δ*::his5*$^{+}$
KLY3828	KLY1546 *cdc5*Δ*::KanMX6 URA3::YFP-CDC10 TRP1::cdc5-3-HA3 bfa1*Δ*::his5*$^{+}$
KLY3832	KLY1546 *cdc5*Δ*::KanMX6 URA3::YFP-CDC10 TRP1::cdc5-3-HA3 bub2*Δ*::his5*$^{+}$
KLY3829	KLY1546 *cdc5*Δ*::KanMX6 URA3::YFP-CDC10 TRP1::cdc5-4-HA3 bfa1*Δ*::his5*$^{+}$
KLY3834	KLY1546 *cdc5*Δ*::KanMX6 URA3::YFP-CDC10 TRP1::cdc5-4-HA3 bub2*Δ*::his5*$^{+}$
KLY3371	KLY1546 *cdc5*Δ*::KanMX6 URA3::YFP-CDC10 TRP1::cdc5-7-HA3 bfa1*Δ*::his5*$^{+}$
KLY3375	KLY1546 *cdc5*Δ*::KanMX6 URA3::YFP-CDC10 TRP1::cdc5-7-HA3 bub2*Δ*::his5*$^{+}$

[a] KLY1546 is in the W303-1A genetic background.

associated kinase activity, the obtained lysates were spun at 15,000 × *g* for 10 min, and the resulting supernatants were subjected to immune complex kinase assays using an anti-HA antibody. Western analyses were carried out with either anti-HA antibody or anti-Cdc28 antibody as described previously (Song *et al.* 2000). Proteins that interact with antibodies were detected by the enhanced chemiluminescence Western detection system (Amersham Biosciences, Piscataway, NJ).

Cell staining and immunofluorescence microscopy: To visualize plasma membranes, cells were stained with DiI (Molecular Probes, Eugene, OR) as described previously (Lippincott and Li 1998a). To determine whether septa are formed between the cell bodies, calcofluor staining was carried out as previously described (Pringle 1991; Lippincott and Li 1998a) with a fluorescent brightener 28 (Sigma), and then serial sections were obtained using a confocal microscope with a 100-nm interval.

Indirect immunofluorescence was performed as described previously (Lee *et al.* 1998). Actin was localized using rhodamine-conjugated phalloidin (Molecular Probes). DNA was visualized with 4′,6-diamidino-2-phenylindole (DAPI). Confocal fluorescent images were collected with a Leica TCS spectrophotometer confocal microscope.

RESULTS

Generation of novel *cdc5* C-terminal domain mutants: Several studies with *cdc5-1* and *msd2-1* mutants have re-

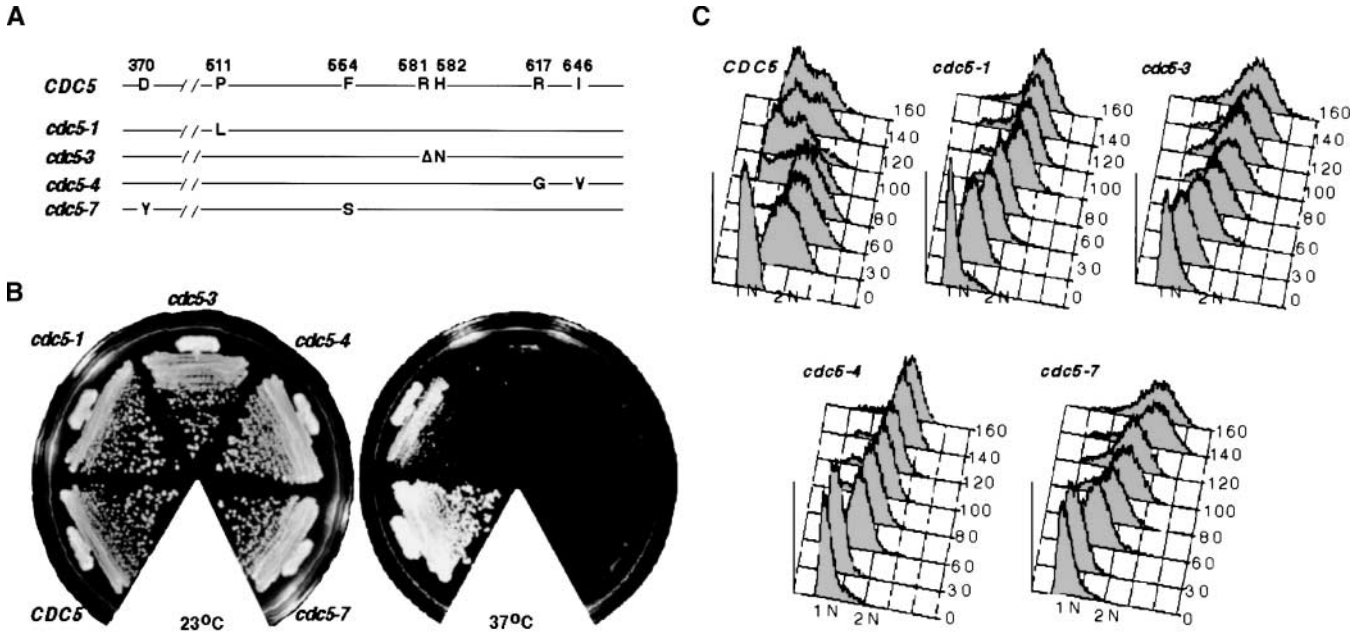

FIGURE 1.—(A) Protein sequence alignment between wild-type Cdc5p and the C-terminal domain mutants. Wild-type amino acid residues and their corresponding mutant residues are shown in the single-letter amino acid code. Numbers in wild-type Cdc5p (*CDC5*) indicate positions of each amino acid residue. Δ, the deletion of R581 residue. (B) Temperature-sensitive growth defect of novel *cdc5* mutants. Cultures were grown on YEP + 2% glucose at the indicated temperature for 3 days. *CDC5*, KLY2470; *cdc5-1*, KLY2458; *cdc5-3*, KLY2460; *cdc5-4*, KLY2462; *cdc5-7*, KLY2464. (C) Flow cytometry analyses of wild-type and *cdc5* mutants. Cells were arrested with α-factor for 3 hr at 23°, washed, and transferred into prewarmed YEP + 2% glucose medium at 37°. Samples were taken at the indicated time points. All the *cdc5* mutants arrest with 2N DNA content, whereas the wild-type strain cycles normally. *CDC5*, KLY2470; *cdc5-1*, KLY2458; *cdc5-3*, KLY2460; *cdc5-4*, KLY2462; *cdc5-7*, KLY2464.

vealed that Cdc5p plays an important role in activating the APC, thereby inactivating Cdc28p/Clb activity (CHARLES *et al.* 1998; SHIRAYAMA *et al.* 1998). In addition, overexpression studies (BARTHOLOMEW *et al.* 2001; SONG and LEE 2001) have suggested that Cdc5p may also contribute to a Swe1p-dependent pathway and to cytokinesis. However, whether Cdc5p contributes to these events under physiological conditions has not been clear. In an attempt to generate novel *cdc5* mutants, defective at a step other than mitotic exit, the C-terminal domain of Cdc5p was mutagenized by PCR and conditional alleles were isolated. Among these, three novel mutants (*cdc5-3*, *cdc5-4*, and *cdc5-7*; Figure 1A) that exhibited a temperature-sensitive cell growth defect (Figure 1B) were chosen for further characterization. Both Cdc5p wild-type and mutant proteins were epitope tagged with three copies of HA to enable immunoprecipitation and detection by immunoblot. The previously characterized *cdc5-1* mutant was used as a comparison. All three mutants grew well at 23°, but they all exhibited a more severe temperature-sensitive growth defect than did the *cdc5-1* mutant at 37° (Figure 1B). To test whether these new *cdc5* alleles were dominant or recessive, each of these mutants was mated with a haploid wild-type strain (KLY1548). The resulting diploids did not exhibit any detectable cell growth or morphological defects at 37° (data not shown), indicating that all three newly generated *cdc5* alleles are recessive. To investigate whether these three mutants have a cell cycle defect similar to that of *cdc5-1*, flow cytometry analyses were carried out. Cells were arrested with α-factor at 23° for 3 hr and then released into fresh medium prewarmed at 37°. Under these conditions, wild-type *CDC5* cells go through the cell cycle normally (Figure 1C). As with the *cdc5-1* mutant, however, all three newly generated *cdc5* mutants were arrested at a point after achieving a 2N DNA content (Figure 1C). Staining of the mutants with DAPI and an antimicrotubule antibody revealed that, as with *cdc5-1*, ~80–90% of these mutant cells were arrested with divided nuclei and elongated spindles upon shifting the temperature to 37° for 3.5 hr (data not shown). These observations suggest that the primary defect of these three mutants is likely to be in exiting mitosis.

To examine the protein expression levels and associated kinase activities of these mutants, Western analyses and immune complex kinase assays were carried out using exponentially growing cells. At the permissive temperature, the expression level of the *cdc5-1* mutant protein was at a level similar to that of wild-type *CDC5*, whereas the expression levels of the *cdc5-3*, *cdc5-4*, and *cdc5-7* mutants were somewhat reduced. At 37°, the steady-state expression levels of the *cdc5-3*, *cdc5-4*, and *cdc5-7* mutants were severalfold lower than that of wild-

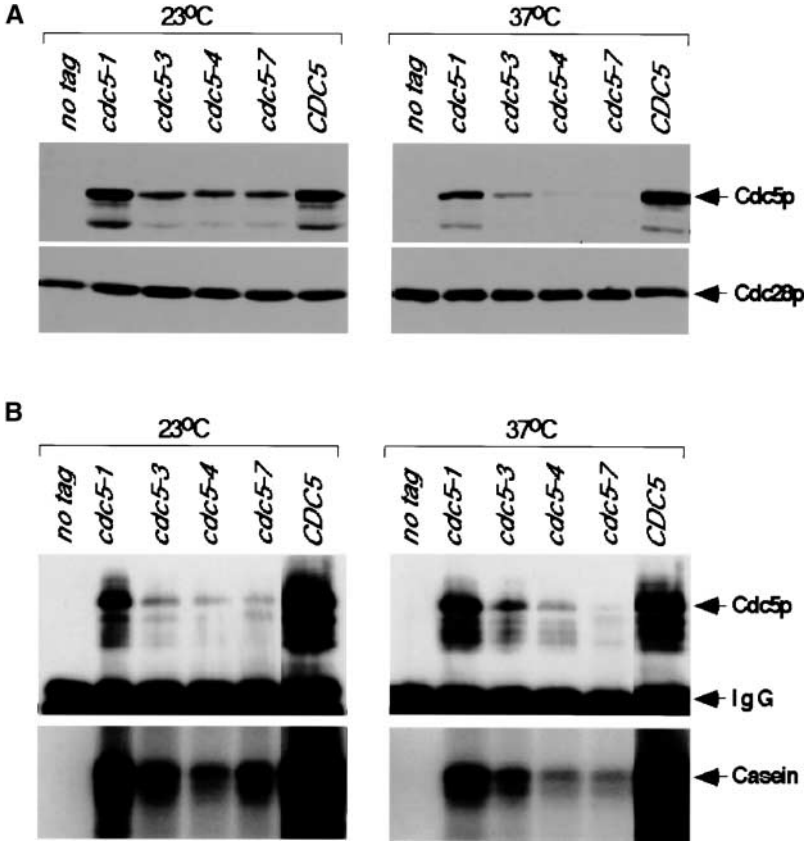

FIGURE 2.—(A) Expression levels of wild-type and *cdc5* mutants. Both Cdc5p wild-type and mutant proteins were epitope tagged with three copies of HA to enable immunoprecipitation and detection by immunoblot (see MATERIALS AND METHODS). Total cellular protein (100 μg of each) was analyzed to determine expression levels of Cdc5p-HA3 with an anti-HA antibody (top) or to determine the level of Cdc28p as an internal loading control (bottom). Lysates were prepared either from cultures grown at 23° (left) or from cultures shifted to 37° for 3.5 hr (right). (B) Kinase activities of wild-type and mutant forms of Cdc5p. Kinase activities were determined by carrying out *in vitro* immune complex kinase assays with supernatants obtained from 15,000 × *g* centrifugation for 15 min (S15). Twenty-eight milligrams of S15 fractions from each mutant were subjected to immunoprecipitation with 5 μg of anti-HA antibody. Levels of immunoprecipitated Cdc5p-HA3 protein were determined by anti-HA Western blotting (top). Kinase activities of various forms of Cdc5p-HA3 were measured using casein as *in vitro* substrate (bottom). no tag, KLY2372 without HA3 tag at the *CDC5* locus; *cdc5-1*, KLY2458; *cdc5-3*, KLY2460; *cdc5-4*, KLY2462; *cdc5-7*, KLY2464; *CDC5*, KLY2470.

type *CDC5* (Figure 2A). Largely consistent with this reduction in protein expression level, the overall kinase activities associated with the cdc5-3p, cdc5-4p, or cdc5-7p immunoprecipitates from equal amounts of each S15 fraction were significantly lower than that of the wild-type Cdc5p at 37° (Figure 2B).

Bypass of mitotic arrest reveals additional defects in *cdc5* mutants: Previous studies with *cdc5* mutants (*cdc5-1* and *msd2-1*) revealed that Cdc5p plays a role in mitotic exit (CHARLES *et al.* 1998; SHIRAYAMA *et al.* 1998). $CDC14^{TAB6\text{-}1}$ was isolated in a genetic screen for *tab* (***t**elophase **a**rrest **b**ypassed*) mutants that bypass the requirement for *CDC15* and *TEM1* function in mitotic exit (SHOU *et al.* 2001). The *cdc5-1* mutant bearing the $CDC14^{TAB6\text{-}1}$ allele grew normally without any apparent defect at 37°, confirming the previous finding that the *cdc5-1* is defective in mitotic exit (Figure 3A). To examine whether the *cdc5-3*, *cdc5-4*, or *cdc5-7* defects could also be alleviated by the $CDC14^{TAB6\text{-}1}$ allele, $CDC14^{TAB6\text{-}1}$ was integrated at the *HIS3* locus. The resulting *cdc5-3* $CDC14^{TAB6\text{-}1}$, *cdc5-4* $CDC14^{TAB6\text{-}1}$, and *cdc5-7* $CDC14^{TAB6\text{-}1}$ strains grew relatively well at 37° (Figure 3A). However, all three mutants exhibited a chained cell morphology to varying degrees and an elongated bud phenotype (see below). Since the *cdc5-1* $CDC14^{TAB6\text{-}1}$ mutant grows normally under these conditions, the slow growth rate of the *cdc5-3* $CDC14^{TAB6\text{-}1}$, *cdc5-4* $CDC14^{TAB6\text{-}1}$, and *cdc5-7* $CDC14^{TAB6\text{-}1}$ mutants suggests that they possess additional uncharacterized defects in addition to the mitotic exit defect.

Cdc5p functions in a Swe1p-dependent Cdc28p/Clb2p activation pathway: To further characterize any additional defects in the *cdc5-3* $CDC14^{TAB6\text{-}1}$, *cdc5-4* $CDC14^{TAB6\text{-}1}$, and *cdc5-7* $CDC14^{TAB6\text{-}1}$ strains, cells were prepared after culturing them at 37° for 3.5 hr. In contrast to *CDC5* $CDC14^{TAB6\text{-}1}$, all three mutants exhibited a significant fraction of cells with large buds (Figure 3B), suggesting that they possess a defect, or defects, at a late stage of the cell cycle. Close examination of cell morphologies after sonication revealed that, unlike the *CDC5* $CDC14^{TAB6\text{-}1}$ and *cdc5-1* $CDC14^{TAB6\text{-}1}$ mutants, all three additional *cdc5* mutants exhibited a chained cell morphology of three to five cell bodies in ~17–20% of the population. In addition to this phenotype, the *cdc5-3* $CDC14^{TAB6\text{-}1}$ strain exhibited an elongated bud morphology in ~13% of the population, whereas other mutants possessed elongated buds in <5% of the total population (Figure 3B). Bud elongation defects occur when yeast cells fail to switch from apical growth to isotropic growth at the time of mitotic onset (BARRAL *et al.* 1999; EDGINGTON *et al.* 1999), a transition that requires a function of the Cdc28p/Clb complex (LEW and REED 1993). Since an elongated bud morphology associated with mutations in the Cdc28p/Clb activation pathway can be prevented by the loss of *SWE1* function (BARRAL *et al.* 1999; EDGINGTON *et al.* 1999; MCMILLAN *et al.* 1999;

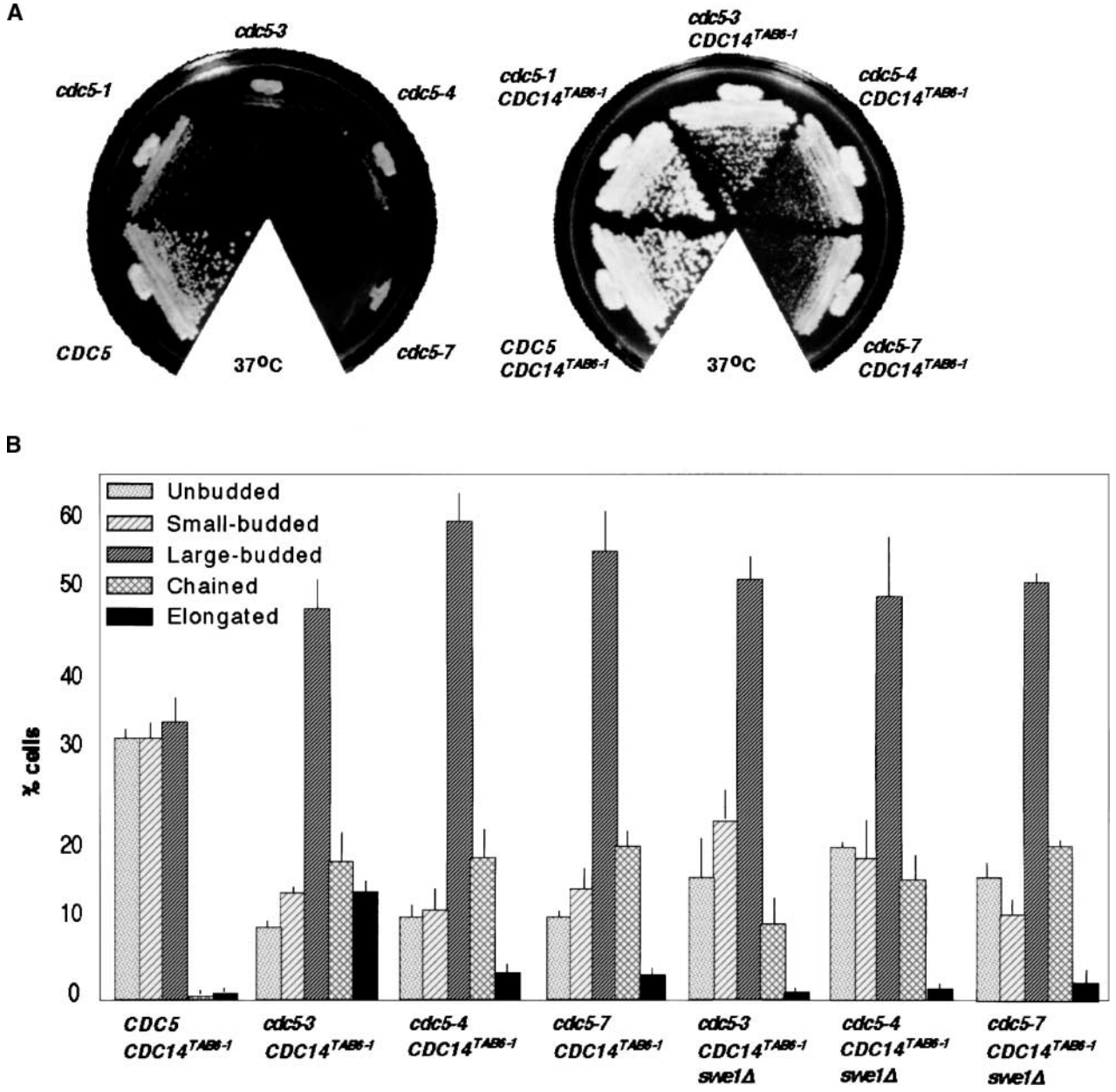

FIGURE 3.—(A) Alleviation of the growth defect of *cdc5* mutants by a dominant allele of *CDC14* (*CDC14*$^{TAB6-1}$). Both wild-type and various *cdc5* mutants were integrated with a dominant *CDC14*$^{TAB6-1}$ allele at the *HIS3* locus and their growth phenotype was examined after culturing the cells on YEP + 2% glucose at 37° for 3 days. (Left) *CDC5*, KLY2470; *cdc5-1*, KLY2458; *cdc5-3*, KLY2460; *cdc5-4*, KLY2462; *cdc5-7*, KLY2464. (Right) *CDC5 CDC14*$^{TAB6-1}$, KLY2970; *cdc5-1 CDC14*$^{TAB6-1}$, KLY2946; *cdc5-3 CDC14*$^{TAB6-1}$, KLY2950; *cdc5-4 CDC14*$^{TAB6-1}$, KLY2954; *cdc5-7 CDC14*$^{TAB6-1}$, KLY2958. (B) Alleviation of elongated bud phenotype by *swe1*Δ. To examine bud elongation in the *swe1*Δ background, *swe1*Δ was introduced into the *cdc5* mutants harboring an integrated copy of the *CDC14*$^{TAB6-1}$ allele. Strains were cultured at 37° for 3.5 hr prior to fixation. The results are the average and standard deviation derived from two independent experiments. More than 300 cells of each sample were counted after sonication. *CDC5 CDC14*$^{TAB6-1}$, KLY2970; *cdc5-3 CDC14*$^{TAB6-1}$, KLY2950; *cdc5-4 CDC14*$^{TAB6-1}$, KLY2954; *cdc5-7 CDC14*$^{TAB6-1}$, KLY2958; *cdc5-3 CDC14*$^{TAB6-1}$ *swe1*Δ, KLY3076; *cdc5-4 CDC14*$^{TAB6-1}$ *swe1*Δ, KLY3122; *cdc5-7 CDC14*$^{TAB6-1}$ *swe1*Δ, KLY3155.

SHULEWITZ *et al.* 1999; LONGTINE *et al.* 2000), a *swe1*Δ mutation was introduced into the three *cdc5* mutants. As expected, introduction of a *swe1*Δ into the *cdc5-3 CDC14*$^{TAB6-1}$ mutant abrogated the elongated bud phenotype; <1% of these cells exhibited an elongated bud morphology after culturing at 37° for 3.5 hr (Figure 3B). In addition, a *swe1*Δ partially alleviated the growth defect of the *cdc5-3 CDC14*$^{TAB6-1}$ mutant (data not shown). Under the same conditions, introduction of a *swe1*Δ into the *CDC5 CDC14*$^{TAB6-1}$ or *cdc5-1 CDC14*$^{TAB6-1}$ strains did not appear to alter the cell morphologies (data not shown).

Since the Hsl1p-Hsl7p pathway plays a critical role in triggering a Swe1p-dependent mitotic delay in response

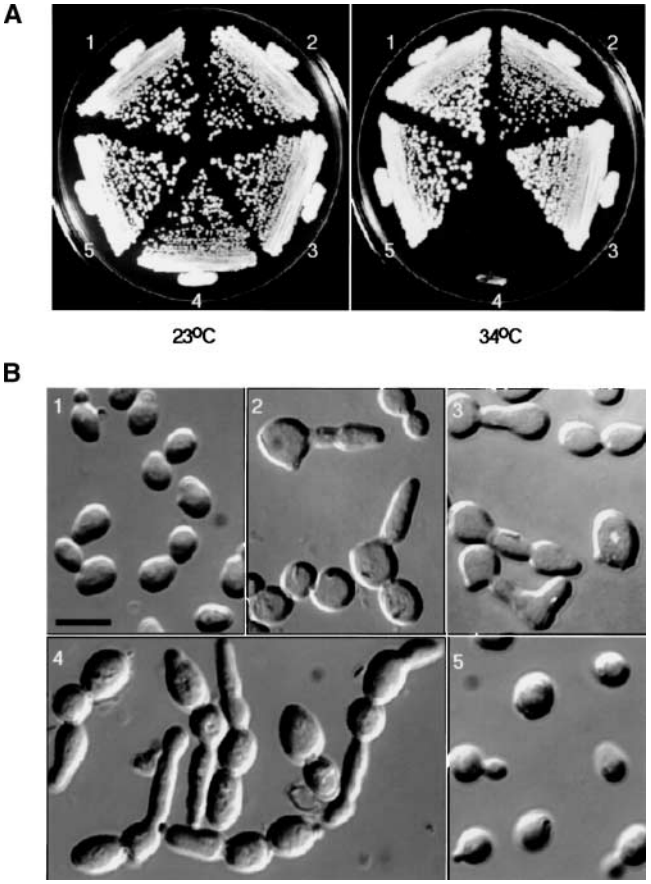

FIGURE 4.—(A) Cdc5p functions in the Swe1p-dependent pathway. Introduction of a *swe1*Δ suppressed the synthetic lethality between *cdc5-3 CDC14*$^{TAB6\text{-}1}$ and *hsl1*Δ. Strains were cultured on YEP + 2% glucose at the indicated temperatures for 3 days. 1, isogenic wild-type KLY1546; 2, KLY3080 (*cdc5-3 CDC14*$^{TAB6\text{-}1}$); 3, KLY2868 (*hsl1*Δ); 4, KLY3170 (*cdc5-3 CDC14*$^{TAB6\text{-}1}$ *hsl1*Δ); 5, KLY3173 (*cdc5-3 CDC14*$^{TAB6\text{-}1}$ *hsl1*Δ *swe1*Δ). (B) Alleviation of enhanced bud elongation defect of the *cdc5-3 CDC14*$^{TAB6\text{-}1}$ *hsl1*Δ mutant by *swe1*Δ. Strains cultured at 23° overnight were shifted to 37° for 3.5 hr and then fixed. Strains used are the same as in A. Bar, 5 μm.

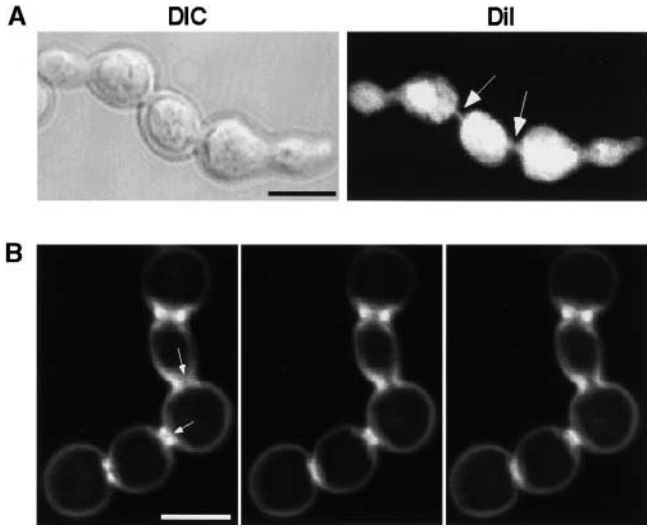

FIGURE 5.—(A) Cytokinetic defect in *cdc5-7 CDC14*$^{TAB6\text{-}1}$ mutant. Strain KLY2958 was cultured in YEP + 2% glucose liquid medium at 23° and then shifted to 37° for an additional 5 hr before fixation with 3.7% formaldehyde. In more than one-half of the connected cell bodies (n = 113) examined, impaired membrane closure was evident by the presence of continuous DiI staining between the cell bodies (arrows). Bar, 5 μm; DIC, differential interference contrast; DiI, DiI staining. (B) Inhibition of septum formation at the internal mother-bud necks. The same samples as in A were stained with calcofluor to reveal septum structure. Cells were then subjected to confocal microscopy with a series of 100-nm sections to examine septum formation between the connected cell bodies. Discontinuous calcofluor signals (arrows) were evident in large fractions (~70%, n = 51) of mother-bud necks of the connected cell bodies, indicating a failure of septum formation. Bar, 5 μm.

to a septin organization defect, we examined whether Cdc5p genetically interacts with this pathway. The *cdc5-3 CDC14*$^{TAB6\text{-}1}$ *hsl1*Δ triple mutant grew slowly at 23°, but failed to grow at 34° (Figure 4A). Upon shifting the cultures to 37° for 3.5 hr, the triple mutant exhibited an enhanced elongated bud morphology when compared to either the *cdc5-3 CDC14*$^{TAB6\text{-}1}$ double or the *hsl1*Δ single mutant (Figure 4B). Under the same conditions, the *cdc5-3 CDC14*$^{TAB6\text{-}1}$ *hsl1*Δ *swe1*Δ mutant grew well with a cellular morphology similar to that of a wild-type strain (Figure 4, A and B). Together, these data suggest that Cdc5p functions at a point upstream of Swe1p, most likely in a pathway distinct from that of Hsl1p and Hsl7p.

Loss of *CDC5* function results in a cytokinetic defect: A defect in cytokinesis may occur as a result of a delay at the G_2/M transition. Thus, we examined the effect of loss of *SWE1* on the cytokinesis defect of various *cdc5* mutants. Introduction of a *swe1*Δ into the *cdc5-4 CDC14*$^{TAB6\text{-}1}$ or *cdc5-7 CDC14*$^{TAB6\text{-}1}$ mutants did not influence the severity of the chained cell morphology, suggesting that this phenotype is not the result of a *SWE1*-dependent cell cycle delay. However, introduction of a *swe1*Δ into the *cdc5-3 CDC14*$^{TAB6\text{-}1}$ mutant decreased, but did not abolish, this phenotype (Figure 3B). To directly investigate cytokinetic defects in these mutants, strains bearing the *CDC14*$^{TAB6\text{-}1}$ allele were grown exponentially at 37° for 5 hr and subjected to DiI staining to reveal the cytoplasmic membrane structures of the connected cells. Under these conditions, ~53% of connected cells (>80 internal mother-bud necks were counted for each mutant, and the peripheral mother-bud necks were excluded from counting) generated from these three mutants (*cdc5-3 CDC14*$^{TAB6\text{-}1}$, *cdc5-4 CDC14*$^{TAB6\text{-}1}$, or *cdc5-7 CDC14*$^{TAB6\text{-}1}$) possessed shared cytoplasm (Figure 5A), suggesting that loss of *CDC5* function resulted in a cytokinetic defect. To visualize chitin deposition and septum formation in the *cdc5* mutants, cells were stained with calcofluor and then subjected to serial optical sectioning using a confocal microscope. Most of the mother-bud necks of connected cells possessed discontinuous calcofluor signals in focal planes bisecting the

cell bodies longitudinally (Figure 5B). These observations, taken together with those obtained by DiI staining, suggest that cytokinesis is either inhibited or delayed in most of the bud necks between connected cell bodies of these *cdc5* mutants.

Aberrant septin function and actin recruitment defect in the *cdc5-4* and the *cdc5-7* mutants: Septins play a critical role in recruiting cytokinetic machinery to the bud neck. They form a ring structure at the future budding site prior to bud emergence. At the time of cytokinesis, this ring disassembles concurrently with spindle disassembly (Lippincott and Li 1998a). To investigate whether the septin structures function normally in the cytokinetically defective *cdc5-7 CDC14^{TAB6-1}* mutant, a *YFP*-fused *CDC10*, a septin component of neck filaments, was integrated into the genome and expressed under native *CDC10* promoter control. When the *CDC5 CDC14^{TAB6-1}* strain was arrested with α-factor for 3 hr at 37° and released into prewarmed medium, cells went through the cell cycle without any noticeable septin defects. In contrast, at 120 min after release, ~25% of the *cdc5-7 CDC14^{TAB6-1}* mutant cells developed a chained cell phenotype with apparent defects in the morphology and subcellular localization of the septin rings. To closely monitor the septin defect in this mutant, cells with three cell bodies were carefully examined as a function of time upon releasing from α-factor block. At 90 min, ~82% of cells with three cell bodies did not exhibit septin rings at the second bud neck. At 180 min, ~52% of these cells exhibited this defect as buds grew. These observations are suggestive of a delay in septin relocalization to, and assembly at, this site (Figure 6, A and B). Consistent with this observation, the percentage of cells with septin rings at both bud necks increased from 18% at 90 min to 43% at 180 min (Figure 6, A and B). A similar septin relocalization/assembly defect was observed in the *cdc5-4 CDC14^{TAB6-1}* mutant (data not shown). Provision of a centromeric *CDC5* plasmid completely rescued this defect (data not shown).

Since the delayed septin relocalization/assembly might have resulted from a defect in septin structure or stability, we carefully examined septin ring morphologies after culturing the cells at 37° for 4 hr. In asynchronously growing cells, ~35% (n = 220) of the *cdc5-4* mutant and 54% (n = 232) of the *cdc5-7* mutant developed abnormally elongated septin rings (Table 2; see the definition of abnormal septin rings in the Figure 6C legend) as evidenced by unusually extended YFP-Cdc10p signals across the mother-bud neck of large-budded cell bodies (Figure 6C). Immunostaining with an anti-Cdc11 antibody resulted in a similar septin ring morphology as visualized with the YFP-Cdc10p fusion protein (data not shown). Provision of a centromeric *CDC5* plasmid completely rescued this defect (data not shown). Under the same conditions, the *cdc5-1* mutant, which is apparently defective only in mitotic exit, possessed aberrant septin rings in <2% (n = 300) of the population. In addition, mitotic exit mutants such as *tem1-3*, *cdc15-2*, and *dbf2-2* did not exhibit this defect (C. J. Park and K. S. Lee, unpublished data). This observation suggests that induction of an aberrant septin ring is not the result of mitotic exit failure and that *cdc5-4* and *cdc5-7* are specifically defective in proper septin structure and function.

To investigate whether the aberrant septin rings are generated at a specific point of the cell cycle, the *cdc5-4* and *cdc5-7* mutants were cultured under various conditions and aberrant septin rings were counted. When cells were arrested with α-factor at 23° and then released to 37° for 4 hr, ~70% of the *cdc5-4* mutant and 80% of the *cdc5-7* mutant exhibited aberrant septin ring morphologies, which was abrogated in the presence of nocodazole (Table 2). Since the *cdc5-4* and *cdc5-7* mutants are also defective in mitotic exit, these observations suggest that aberrant septin rings are induced at a point after the nocodazole block, but prior to mitotic exit. Consistent with this notion, both the *cdc5-4* and the *cdc5-7* mutants bearing the *CDC14^{TAB6-1}* allele (*cdc5-4 CDC14^{TAB6-1}* and *cdc5-7 CDC14^{TAB6-1}*, respectively) exhibited significantly decreased aberrant septin structures under the same culture conditions (Table 2).

Since septin ring structure is pivotal for recruiting cytokinetic machinery, the observed defect in septin structure and function may have directly contributed to the cytokinesis defect. Thus, we examined actin localization in cells with fully elongated spindles. Approximately 54% (n = 220) of the *cdc5-4 CDC14^{TAB6-1}* mutant and 46% (n = 216) of the *cdc5-7 CDC14^{TAB6-1}* mutant possessed visible actin rings after 4 hr at 37°, whereas 87% (n = 187) of the *CDC5 CDC14^{TAB6-1}* mutant possessed distinct actin rings under the same conditions (Table 3). Taken together, it is likely that a defect in septin function in the *cdc5-4* and *cdc5-7* mutants may have resulted in delayed actin recruitment leading to a cytokinetic defect.

Cdc5p contributes to cytokinesis independently of Bfa1p and Bub2p: It has been recently demonstrated that Cdc5p contributes to the phosphorylation of Bfa1p *in vivo* (Hu *et al.* 2001; Lee *et al.* 2001b), suggesting that Cdc5p controls the MEN by directly regulating Bfa1p function. Since the MEN is required for normal cytokinesis (Jimenez *et al.* 1998; Frenz *et al.* 2000; Lee *et al.* 2001a), we investigated whether the cytokinetic defect associated with the *cdc5-4* and *cdc5-7* mutants is due to a failure to negatively regulate the Bfa1p/Bub2p-dependent inhibition of the MEN. As observed with the provision of *CDC14^{TAB6-1}*, introduction of a *bfa1*Δ or a *bub2*Δ suppressed the growth defect of all four *cdc5* mutants (*cdc5-1*, *cdc5-3*, *cdc5-4*, and *cdc5-7*) at 37° (data not shown). However, a *bfa1*Δ or a *bub2*Δ failed to sup-

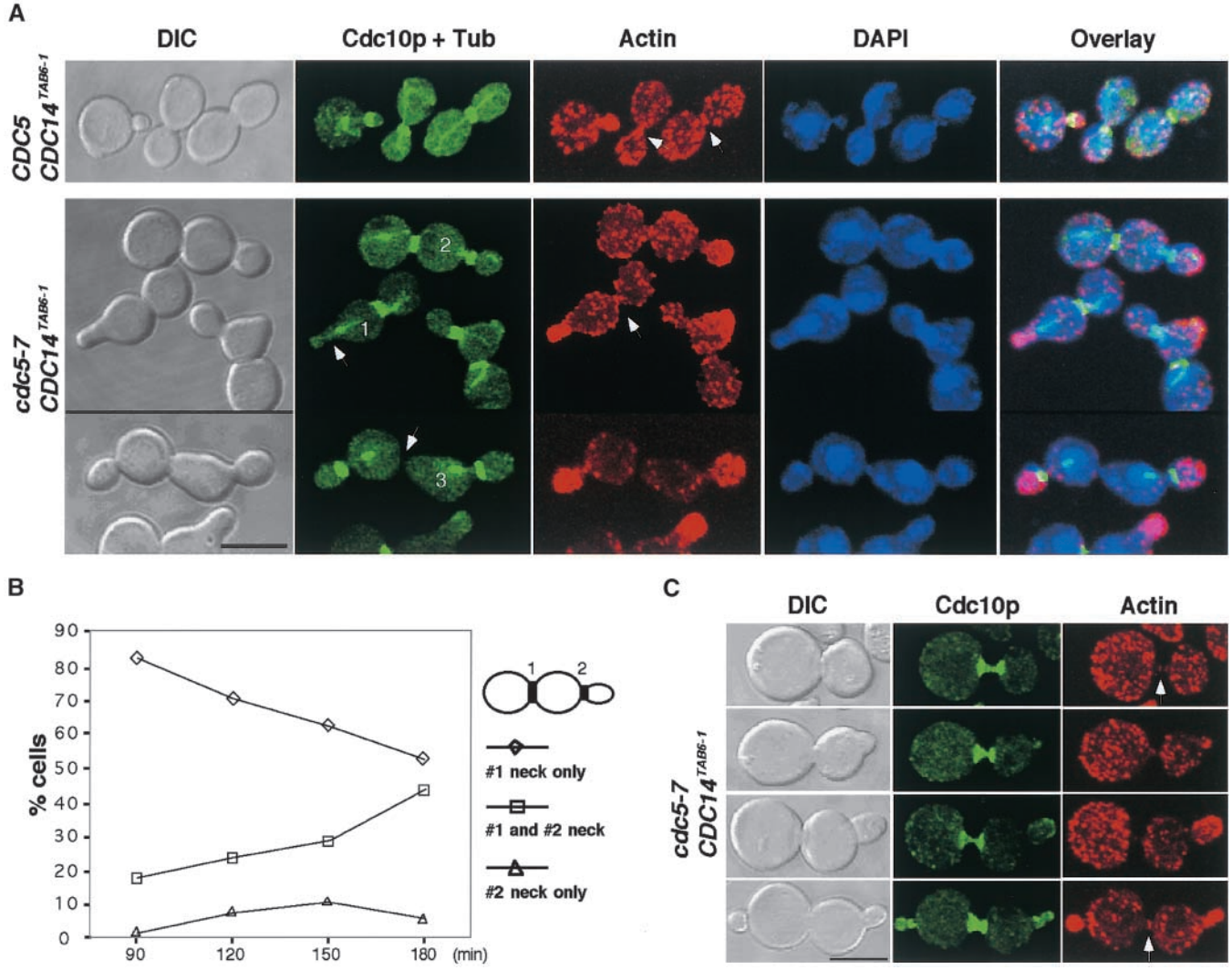

FIGURE 6.—Aberrant septin function in a *cdc5-7 CDC14*$^{TAB6-1}$ mutant. (A) The *cdc5-7 CDC14*$^{TAB6-1}$ mutant expressing *YFP-CDC10* under its native promoter (KLY3072) was arrested in G_1 with α-factor at 37° for 3 hr. Upon releasing these cells into fresh medium prewarmed at 37°, cells were harvested at the indicated time points and sonicated prior to examining the septin ring morphologies. A large fraction of cells at 150 min (61%, $n = 203$) did not possess readily visible septin rings at the second mother-bud necks with small buds (arrow in no. 1 cell of Cdc10p + Tub panel). In addition, ~30% ($n = 205$) of cells possessed second septin rings in the absence of disassembly of the first septin ring (no. 2 cell of Cdc10p + Tub panel). More than 98% ($n = 150$) of the cells with four or more cell bodies did not possess septin rings at the first cytokinetic sites (arrow in no. 3 cell of Cdc10p + Tub panel). Recruited actin rings (arrows in the Actin panel) were rarely visible in the connected cells, suggesting that these cell bodies are still capable of recruiting cytokinetic machineries. Under the same conditions, the *CDC5 CDC14*$^{TAB6-1}$ strain (KLY3075) did not exhibit any noticeable septin defect (top). A copy of a *TUB-GFP* fusion was additionally integrated to visualize the cell cycle stages of individual cell bodies in the connected cells. DIC, differential interference contrast; Cdc10p + Tub, YFP-Cdc10p + GFP-tubulin; Actin, actin-phalloidin staining; DAPI, DNA staining. Superimposed images are shown in overlays. Bar, 5 μm. (B) Quantification of cells with aberrant septin rings in the *cdc5-7 CDC14*$^{TAB6-1}$ mutant. Cells defective in septin disassembly or assembly were quantified using the same samples prepared in A. Approximately 200 cells with three cell bodies were counted at each time point. Cells were classified into three groups: septin ring at the first bud neck (no. 1 neck only), at the first and second bud necks (no. 1 and no. 2 neck), and at the second neck (no. 2 neck only). Percentages of cells in each group were determined at each time point and plotted as a function of time after release from α-factor block. (C) The *cdc5-7 CDC14*$^{TAB6-1}$ (strain KLY3578) cells grown at 23° were shifted to 37° for 4 hr and then harvested to examine the septin ring morphologies. In ~23% ($n = 1261$) of the population, septin rings are loosely organized, as revealed by YFP-Cdc10p signals. Septin rings are considered aberrant when the width (the longitudinal length that spans the two cell bodies) is longer than the height (the length along the mother-bud neck). Weak actin bars (arrows) were still visible in 65% ($n = 212$) of the cells with aberrant septin rings. Bar, 5 μm.

press the chained cell phenotype of the *cdc5-3*, *cdc5-4*, and *cdc5-7* mutants, when compared with the respective mutants bearing the *CDC14*$^{TAB6-1}$ allele (Table 4). In addition, DiI staining revealed that, among the chained cells, ~40% of the *cdc5-7 bfa1*Δ and *cdc5-7 bub2*Δ mutants possessed connected cytoplasms (data not shown).

TABLE 2

Induction of aberrant septin ring structures in the *cdc5-4* and *cdc5-7* mutants occurs prior to mitotic exit

	CDC5	*CDC5 CDC14^{TAB6-1}*	*cdc5-4*	*cdc5-4 CDC14^{TAB6-1}*	*cdc5-7*	*cdc5-7 CDC14^{TAB6-1}*
% asynchronous	0.0	0.0	35.3	9.5	54.2	20.8
% α → release	0.0	0.0	70.3	35.8	80.3	47.2
% α → noc	0.0	0.0	0.8	0.5	2.1	5.2

To prepare randomly growing samples, cells grown at 23° were shifted to 37° for 4 hr prior to fixation. For α-factor-treated samples, cells were cultured in the presence of α-factor for 2.5 hr at 23° and then released into either prewarmed fresh medium or nocodazole-containing medium for an additional 4 hr at 37°. Both α-factor and nocodazole were used at the concentration of 15 μg/ml. *CDC5*, KLY3209; *CDC5 CDC14^{TAB6-1}*, KLY3075; *cdc5-4*, KLY3205; *cdc5-4 CDC14^{TAB6-1}*, KLY3071; *cdc5-7*, KLY3206; *cdc5-7 CDC14^{TAB6-1}*, KLY3072.

These observations suggest that Cdc5p contributes to cytokinesis independently of the Bfa1p/Bub2p-dependent regulation of the MEN.

DISCUSSION

Data obtained from various organisms suggest that polo kinases play important roles at multiple points of M-phase progression and that their roles are largely conserved among evolutionarily distant organisms. In budding yeast, ectopic expression of the mammalian polo-like kinase *PLK1* complements the mitotic exit defect associated with the *cdc5-1* mutation (Lee and Erikson 1997), indicating that at least polo kinase-dependent APC activation is conserved between budding yeast and mammals. Studies with a dominant-negative *cdc5* mutant (Song and Lee 2001) and the work reported here suggest that, like the proposed cytokinetic roles of polo kinases in other eukaryotic organisms (Ohkura *et al.* 1995; Mundt *et al.* 1997; Adams *et al.* 1998; Bahler *et al.* 1998; Carmena *et al.* 1998), Cdc5 is required for normal cytokinesis.

Besides its roles in mitotic exit and cytokinesis, Cdc5p has also been implicated in the regulation of Swe1p. Bartholomew *et al.* (2001) have reported that overexpression of wild-type *CDC5* or kinase-inactive *CDC5/N209A* under control of the *GAL1* promoter leads to Swe1p phosphorylation. In addition, expression of *GAL1-CDC5/N209A* suppresses Swe1p-dependent elongated bud formation in *hsl1* or *hsl7* mutants (Bartholomew *et al.* 2001). These authors have suggested that Cdc5p may function as a negative regulator of Swe1p (Bartholomew *et al.* 2001). In support of this notion, we have observed that the *cdc5-3 CDC14^{TAB6-1}* mutant exhibits an elongated bud phenotype. The *cdc5-3 CDC14^{TAB6-1} hsl1*Δ triple mutant exhibited enhanced bud elongation and synthetic lethality at 34°. Introduction of a *swe1*Δ into the *cdc5-3 CDC14^{TAB6-1} hsl1*Δ mutant abrogated this elongated bud phenotype and suppressed the growth defect, indicating that Cdc5p functions in the Swe1p-dependent checkpoint pathway. Defects in septin assembly cause a G_2 delay, resulting in a filamentous phenotype (Barral *et al.* 1999; Edgington *et al.* 1999; Shulewitz *et al.* 1999; Longtine *et al.* 2000). However, only 3% (n = 355) of the *cdc5-3 CDC14^{TAB6-1}* mutant exhibited aberrant septin ring structures, in comparison to 21% (n = 260) of the *cdc5-7 CDC14^{TAB6-1}* mutant under the same conditions. In addition, the *cdc5-4 CDC14^{TAB6-1}* and *cdc5-7 CDC14^{TAB6-1}* mutants, which possess a gross septin defect, exhibited fewer cells with elongated buds than did the *cdc5-3 CDC14^{TAB6-1}* mutant. These observations suggest that the elongated bud morphology in the *cdc5-3 CDC14^{TAB6-1}* mutant may likely be due to a defect in mediating the septin-dependent inactivation of Swe1p rather than to an indirect septin perturbation effect. How Cdc5p relates its activity to other regulatory components of the Swe1p-dependent pathway and regulates the activation of Cdc28p/Clb remains to be investigated further.

The *cdc5-4 CDC14^{TAB6-1}* mutant and the *cdc5-7 CDC-*

TABLE 3

Actin localization defect in *cdc5* mutants

	CDC5 CDC14^{TAB6-1}	*cdc5-1 CDC14^{TAB6-1}*	*cdc5-3 CDC14^{TAB6-1}*	*cdc5-4 CDC14^{TAB6-1}*	*cdc5-7 CDC14^{TAB6-1}*
% cells with localized actin	87.1	75.9	56.1	54.3	46.1

Cells were grown at 23° and then shifted to 37° for 3.5 hr prior to fixation. After sonication, ~200 cells with elongated spindles were counted to determine the percentage of cells with localized actins at the bud neck. *CDC5 CDC14^{TAB6-1}*, KLY2970; *cdc5-1 CDC14^{TAB6-1}*, KLY2946; *cdc5-3 CDC14^{TAB6-1}*, KLY2950; *cdc5-4 CDC14^{TAB6-1}*, KLY2954; *cdc5-7 CDC14^{TAB6-1}*, KLY2958.

TABLE 4

A Bfa1p/Bub2p-independent cytokinesis defect in *cdc5* mutants

	% chained cells
CDC5	0.2
CDC5 CDC14^{TAB6-1}	0.0
*CDC5 bfa1*Δ	0.6
*CDC5 bub2*Δ	3.2
cdc5-1 CDC14^{TAB6-1}	3.4
*cdc5-1 bfa1*Δ	3.7
*cdc5-1 bub2*Δ	6.9
cdc5-3 CDC14^{TAB6-1}	13.5
*cdc5-3 bfa1*Δ	23.7
*cdc5-3 bub2*Δ	24.5
cdc5-4 CDC14^{TAB6-1}	18.0
*cdc5-4 bfa1*Δ	28.3
*cdc5-4 bub2*Δ	28.5
cdc5-7 CDC14^{TAB6-1}	25.4
*cdc5-7 bfa1*Δ	36.1
*cdc5-7 bub2*Δ	39.1

Cells were grown at 23° and then shifted to 37° for 3.5 hr prior to fixation. After sonication, >300 cells were counted to determine the percentage of cells with connected cell bodies (% chained cells). Cells with more than three cell bodies were counted as chained cells. *CDC5*, KLY2470; *CDC5 CDC14^{TAB6-1}*, KLY2970; *CDC5 bfa1*Δ, KLY2374; *CDC5 bub2*Δ, KLY2573; *cdc5-1 CDC14^{TAB6-1}*, KLY2946; *cdc5-1 bfa1*Δ, KLY3826; *cdc5-1 bub2*Δ, KLY3831; *cdc5-3 CDC14^{TAB6-1}*, KLY2950; *cdc5-3 bfa1*Δ, KLY3828; *cdc5-3 bub2*Δ, KLY3832; *cdc5-4 CDC14^{TAB6-1}*, KLY2954; *cdc5-4 bfa1*Δ, KLY3829; *cdc5-4 bub2*Δ, KLY3834; *cdc5-7 CDC14^{TAB6-1}*, KLY2958; *cdc5-7 bfa1*Δ, KLY3371; *cdc5-7 bub2*Δ, KLY3375.

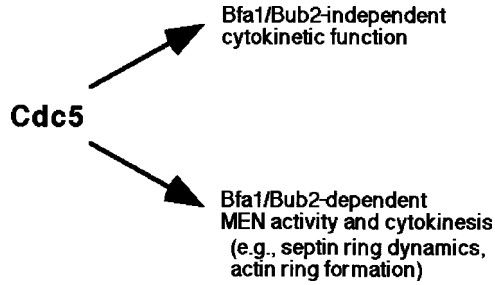

Figure 7.—Model proposing the Bfa1p/Bub2p-independent cytokinetic role of Cdc5p. Cdc5p regulates Bfa1p/Bub2p-dependent MEN activity, which is also shown to be important for septin ring dynamics (Lippincott *et al.* 2001) and actin ring formation (Frenz *et al.* 2000; Lee *et al.* 2001a). The data reported here show that the *cdc5-7* mutant exhibits a cytokinetic defect even in the absence of Bfa1p or Bub2p, indicating the presence of a Bfa1p/Bub2p-independent cytokinetic pathway.

14^{TAB6-1} mutant displayed delayed septin localization to the incipient bud site in chained cells. These mutants also exhibited aberrant septin ring morphologies, as evidenced by the presence of loosely organized YFP-Cdc10p signals at the bud necks. However, these mutants did not appear to possess a significant defect in the G_2/M transition, as judged by lack of an elongated bud morphology at the restrictive temperature. These observations suggest that the apparent septin defect in these mutants is not sufficient to trigger a G_2 delay, although it may be sufficient to contribute to the cytokinetic failure. Close examination of septin structures in the *cdc5-4* and *cdc5-7* mutants revealed that a high percentage of aberrant septin rings is induced between early mitosis and mitotic exit, a period in which septin disassembly and relocalization do not occur. In contrast, aberrant septin structures were not observed in other mutants in the MEN such as *tem1-3*, *cdc15-2*, or *dbf2-2* (C. J. Park and K. S. Lee, unpublished data). These observations suggest that a Cdc5p-dependent mitotic activity is likely to be important for proper septin function and therefore for normal cytokinesis. In addition, a relatively low penetrant defect associated with the *cdc5-4* or *cdc5-7* mutation suggests that alternative pathway(s) may exist to compensate the cytokinetic defect associated with these mutations. In support of this argument, the *cdc5-3* mutant with largely normal septin ring structures (3% of aberrant septin rings in *cdc5-3 CDC14^{TAB6-1}* as opposed to 21% in *cdc5-7 CDC14^{TAB6-1}* as judged by fluorescent YFP-Cdc10p signals at the neck) still exhibits a significant cytokinetic defect even in the *swe1*Δ background (Figure 3B). Although it may be difficult to assess the functionality of septins by neck-localized YFP-Cdc10p signals, this observation suggests the possibility of a septin-organization-independent cytokinesis failure in this mutant. A deeper understanding of how Cdc5p contributes to normal cytokinesis and septin function may require identification of additional Cdc5p interacting proteins and physiological substrates important for this event.

Recent reports have shown that mutations in components of the MEN such as Cdc5p, Tem1p, Cdc15p, Dbf2p, and Cdc14p result in a defect in actin ring formation (Frenz *et al.* 2000; Lee *et al.* 2001a). In addition, Lippincott *et. al.* (2001) have reported that the *tem1*$^-$ mutant exhibits a defect in the actin ring and septin ring dynamics, when its mitotic exit defect is alleviated. Cdc5p has been shown to phosphorylate and negatively regulate Bfa1p (Hu *et al.* 2001), which may form a two-component GAP with Bub2p for the Tem1p GTPase. In an attempt to examine whether the cytokinetic defect of *cdc5-4* and *cdc5-7* could be the result of a failure to regulate Bfa1p/Bub2p properly, we examined whether introduction of a *bfa1*Δ or a *bub2*Δ alleviates the cytokinetic defect associated with loss of *CDC5* function. We found that introduction of a *bfa1*Δ or a *bub2*Δ into the *cdc5* mutants resulted in a degree of cytokinetic defect similar to that resulting from the introduction of *CDC14^{TAB6-1}*. These observations indicate that the cytokinetic defect associated with the loss of *CDC5* function is independent of Bfa1p/Bub2p function or activity (Figure 7). However, whether or not Cdc5p contributes to cytokinesis by activating the MEN downstream of

Tem1p is not yet clear. Recently, Lee *et al.* (2001a) have shown that Cdc5p is required for Dbf2p kinase activity even in the absence of Bub2p, suggesting that Cdc5p may also contribute to Dbf2p activity through a Bfa1p/Bub2p-independent pathway. Whether Cdc5p contributes to the regulation of cytokinesis by directly regulating Dbf2p activity or by a yet-unidentified pathway requires further investigation (Figure 7).

Data obtained from various organisms show that polo kinases play multiple roles during M-phase progression. In mammalian cells, Plk localizes at centrosomes in G_2 and early mitosis and at the midbody in late mitosis and cytokinesis. The C-terminal domain of Plk is sufficient to localize at these sites (Y. S. Seong and K. S. Lee, unpublished data). In budding yeast, Cdc5p localizes at the spindle pole bodies. Later in the cell cycle, Cdc5p localizes to bud neck in both the polo-box- and the septin-dependent manner (Song and Lee 2001; C. J. Park and K. S. Lee, unpublished data). The dynamic subcellular localization of polo kinases presages their diverse functions in various organisms. The data presented here suggest that the C-terminal domain of Cdc5p is required for interacting with various physiological binding partners important for G_2/M transition, mitotic exit, and cytokinesis. Although the morphological features and timing of certain events during M-phase progression are strikingly different between budding yeast and mammalian cells, spatial regulation of polo kinases may be critical for coordinating multiple mitotic events in all eukaryotes.

We are grateful to Dan Ilkovitch for technical support. We thank Jeremy Thorner (University of California-Berkeley) for providing the *hsl1*Δ strain, Susan Garfield for helping with confocal microscopy, and Jim McNally and Tatiana Kapova for processing confocal images obtained at the LRBGE Fluorescence Imaging Facility in NCI/DBS.

LITERATURE CITED

Adams, R., A. Tavares, A. Salzberg, H. Bellen and D. Glover, 1998 *pavarotti* encodes a kinesin-like protein required to organize the central spindle and contractile ring for cytokinesis. Genes Dev. **12:** 1483–1494.

Bahler, J., A. B. Steever, S. Wheatley, Y. I. Wang, J. R. Pringle *et al.*, 1998 Role of polo kinase and Mid1p in determining the site of cell division in fission yeast. J. Cell Biol. **143:** 1603–1616.

Barral, Y., M. Parra, S. Bidlingmaier and M. Snyder, 1999 Nim1-related kinases coordinate cell cycle progression with the organization of the peripheral cytoskeleton in yeast. Genes Dev. **13:** 176–187.

Barral, Y., V. Mermall, M. S. Mooseker and M. Snyder, 2000 Compartmentalization of the cell cortex by septins is required for maintenance of cell polarity in yeast. Mol. Cell **5:** 841–851.

Bartholomew, C. R., S. H. Woo, Y. S. Chung, C. Jones and C. F. Hardy, 2001 Cdc5 interacts with the wee1 kinase in budding yeast. Mol. Cell. Biol. **21:** 4949–4959.

Bi, E., P. Maddox, D. J. Lew, E. D. Salmon, J. N. McMillan *et al.*, 1998 Involvement of an actomyosin contractile ring in *Saccharomyces cerevisiae* cytokinesis. J. Cell Biol. **142:** 1301–1312.

Booher, R. N., R. J. Deshaies and M. W. Kirschner, 1993 Properties of *Saccharomyces cerevisiae* wee1 and its differential regulation of p34CDC28 in response to G1 and G2 cyclins. EMBO J. **12:** 3417–3426.

Carmena, M., M. G. Riparbelli, G. Minestrini, A. M. Tavares, R. Adams *et al.*, 1998 *Drosophila* polo kinase is required for cytokinesis. J. Cell Biol. **143:** 659–671.

Carroll, C. W., R. Altman, D. Schieltz, J. R. Yates and D. Kellogg, 1998 The septins are required for the mitosis-specific activation of the Gin4 kinase. J. Cell Biol. **143:** 709–717.

Chant, J., M. Mischke, E. Mitchell, I. Herskowitz and J. R. Pringle, 1995 Role of Bud3p in producing the axial budding pattern of yeast. J. Cell Biol. **129:** 767–778.

Charles, J., S. Jaspersen, R. Tinker-Kulberg, L. Hwang, A. Szidon *et al.*, 1998 The Polo-related kinase Cdc5 activates and is destroyed by the mitotic cyclin destruction machinery in *S. cerevisiae*. Curr. Biol. **8:** 497–507.

DeMarini, D. J., A. E. Adams, H. Fares, C. D. Virgilio, G. Valle *et al.*, 1997 A septin-based hierarchy of proteins required for localized deposition of chitin in the *Saccharomyces cerevisiae* cell wall. J. Cell Biol. **139:** 75–93.

Descombes, P., and E. A. Nigg, 1998 The polo-like kinase Plx1 is required for M phase exit and destruction of mitotic regulators in *Xenopus* egg extracts. EMBO J. **17:** 1328–1335.

Edgington, N. P., M. J. Blacketer, T. A. Bierwagen and A. M. Myers, 1999 Control of *Saccharomyces cerevisiae* filamentous growth by cyclin-dependent kinase Cdc28. Mol. Cell. Biol. **19:** 1369–1380.

Frazier, J. A., M. L. Wong, M. S. Longtine, J. R. Pringle, M. Mann *et al.*, 1998 Polymerization of purified yeast septins: evidence that organized filament arrays may not be required for septin function. J. Cell Biol. **143:** 737–749.

Frenz, L. M., S. E. Lee, D. Fesquet and L. H. Johnston, 2000 The budding yeast Dbf2 protein kinase localises to the centrosome and moves to the bud neck in late mitosis. J. Cell Sci. **19:** 3399–3408.

Furge, K. A., K. Wong, J. Armstrong, M. Balasubramanian and C. F. Albright, 1998 Byr4 and Cdc16 form a two-component GTPase-activating protein for the Spg1 GTPase that controls septation in fission yeast. Curr. Biol. **8:** 947–954.

Giot, L., and J. B. Konopka, 1997 Functional analysis of the interaction between Afr1p and the Cdc12p septin, two proteins involved in pheromone-induced morphogenesis. Mol. Biol. Cell **8:** 987–998.

Glover, D. M., I. M. Hagan and A. A. M. Tavares, 1998 Polo-like kinases: a team that plays throughout mitosis. Genes Dev. **12:** 3777–3787.

Hu, F., Y. Wang, D. Liu, Y. Li, J. Qin *et al.*, 2001 Regulation of the Bub2/Bfa1 GAP complex by Cdc5 and cell cycle checkpoints. Cell **107:** 655–665.

Ito, H., Y. Fukuda, K. Murata and A. Kimura, 1983 Transformation of intact yeast cells treated with alkali cations. J. Bacteriol. **153:** 163–168.

Jimenez, J., V. J. Cid, R. Cenamor, M. Yuste, G. Molero *et al.*, 1998 Morphogenesis beyond cytokinetic arrest in *Saccharomyces cerevisiae*. J. Cell Biol. **143:** 1617–1634.

Kumagai, A., and W. G. Dunphy, 1996 Purification and molecular cloning of Plx1, a Cdc25-regulatory kinase from *Xenopus* egg extracts. Science **273:** 1377–1380.

Lane, H., and E. A. Nigg, 1997 Cell-cycle control: POLO-like kinases join the outer circle. Trends Cell Biol. **7:** 63–68.

Lee, K. S., and R. L. Erikson, 1997 Plk is a functional homolog of *Saccharomyces cerevisiae* Cdc5, and elevated Plk activity induces multiple septation structures. Mol. Cell. Biol. **17:** 3408–3417.

Lee, K. S., T. Z. Grenfell, F. R. Yarm and R. L. Erikson, 1998 Mutation of the polo-box disrupts localization and mitotic functions of the mammalian polo kinase Plk. Proc. Natl. Acad. Sci. USA **95:** 9301–9306.

Lee, K. S., S. Song and R. L. Erikson, 1999 The polo-box-dependent induction of ectopic septal structures by a mammalian polo kinase, Plk, in *Saccharomyces cerevisiae*. Proc. Natl. Acad. Sci. USA **96:** 14360–14365.

Lee, S. E., L. M. Frenz, N. J. Wells, A. L. Johnson and L. H. Johnston, 2001a Order of function of the budding-yeast mitotic exit-network proteins Tem1, Cdc15, Mob1, Dbf2, and Cdc5. Curr. Biol. **11:** 784–788.

Lee, S. E., S. Jensen, L. M. Frenz, A. L. Johnson, D. Fesquet *et al.*, 2001b The Bub2-dependent mitotic pathway in yeast acts every cell cycle and regulates cytokinesis. J. Cell Sci. **114:** 2345–2354.

Lew, D. J., and S. I. Reed, 1993 Morphogenesis in the yeast cell cycle: regulation by Cdc28 and cyclins. J. Cell Biol. **120:** 1305–1320.

Lippincott, J., and R. Li, 1998a Dual function of Cyk2, a cdc15/PSTPIP family protein, in regulating actomyosin ring dynamics and septin distribution. J. Cell Biol. **143:** 1947–1960.

Lippincott, J., and R. Li, 1998b Sequential assembly of myosin II, an IQGAP-like protein, and filamentous actin to a ring structure involved in budding yeast cytokinesis. J. Cell Biol. **140:** 355–366.

Lippincott, J., K. B. Shannon, W. Shou, R. J. Deshaies and R. Li, 2001 The Tem1 small GTPase controls actomyosin and septin dynamics during cytokinesis. J. Cell Sci. **114:** 1379–1386.

Longtine, M. S., D. J. DeMarini, M. L. Valencik, O. S. Al-Awar, H. Fares *et al.*, 1996 The septins: roles in cytokinesis and other processes. Curr. Opin. Cell Biol. **8:** 106–119.

Longtine, M. S., A. McKenzie, D. J. DeMarini, N. G. Shah, A. Wach *et al.*, 1998 Additional modules for versatile and economical PCR-based gene deletion and modification in *Saccharomyces cerevisiae*. Yeast **14:** 953–961.

Longtine, M. S., C. L. Theesfeld, J. N. McMillan, E. Weaver, J. R. Pringle *et al.*, 2000 Septin-dependent assembly of a cell cycle-regulatory module in *Saccharomyces cerevisiae*. Mol. Cell. Biol. **20:** 4049–4061.

Ma, X. J., Q. Lu and M. Grunstein, 1996 A search for proteins that interact genetically with histone H3 and H4 amino termini uncovers novel regulators of the Swe1 kinase in *Saccharomyces cerevisiae*. Genes Dev. **10:** 1327–1340.

McMillan, J. N., M. S. Longtine, R. A. Sia, C. L. Theesfeld, E. S. Bardes *et al.*, 1999 The morphogenesis checkpoint in *Saccharomyces cerevisiae*: cell cycle control of Swe1p degradation by Hsl1p and Hsl7p. Mol. Cell. Biol. **19:** 6929–6939.

Muhlrad, D., R. Hunter and R. Parker, 1992 A rapid method for localized mutagenesis of yeast genes. Yeast **8:** 79–82.

Mundt, K. E., R. M. Golsteyn, H. A. Lane and E. A. Nigg, 1997 On the regulation and function of human polo-like kinase 1(PLK1): effects of overexpression on cell cycle progression. Biochem. Biophys. Res. Commun. **239:** 377–385.

Ohkura, H., I. M. Hagan and D. M. Glover, 1995 The conserved *Schizosaccharomyces pombe* kinase plo1, required to form a bipolar spindle, the actin ring, and septum, can drive septum formation in G1 and G2 cells. Genes Dev. **9:** 1059–1073.

Pringle, J. R., 1991 Staining of bud scars and other cell wall chitin with calcofluor. Methods Enzymol. **194:** 732–735.

Sherman, F., G. R. Fink and J. B. Hicks, 1986 *Methods in Yeast Genetics*. Cold Spring Harbor Laboratory Press, Cold Spring Harbor, NY.

Shirayama, M., W. Zachariae, R. Ciosk and K. Nasmyth, 1998 The Polo-like kinase Cdc5p and the WD-repeat protein Cdc20p/fizzy are regulators and substrates of the anaphase promoting complex in *Saccharomyces cerevisiae*. EMBO J. **17:** 1336–1349.

Shou, W., K. M. Sakamoto, J. Keener, K. W. Morimoto, E. E. Traverso *et al.*, 2001 Net1 stimulates RNA polymerase I transcription and regulates nucleolar structure independently of controlling mitotic exit. Mol. Cell **8:** 45–55.

Shulewitz, M. J., C. J. Inouye and J. Thorner, 1999 Hsl7 localizes to a septin ring and serves as an adapter in a regulatory pathway that relieves tyrosine phosphorylation of Cdc28 protein kinase in *Saccharomyces cerevisiae*. Mol. Cell. Biol. **19:** 7123–7137.

Song, S., and K. S. Lee, 2001 A novel function of *Saccharomyces cerevisiae CDC5* in cytokinesis. J. Cell Biol. **152:** 451–469.

Song, S., T. Z. Grenfell, S. Garfield, R. L. Erikson and K. S. Lee, 2000 Essential function of the polo box of Cdc5 in subcellular localization and induction of cytokinetic structures. Mol. Cell. Biol. **20:** 286–298.

Takizawa, P. A., J. L. DeRisi, J. E. Wilhelm and R. D. Vale, 2000 Plasma membrane compartmentalization in yeast by messenger RNA transport and a septin diffusion barrier. Science **290:** 341–344.

Tanaka, K., J. Petersen, F. MacIver, D. P. Mulvihill, D. M. Glover *et al.*, 2001 The role of Plo1 kinase in mitotic commitment and septation in *Schizosaccharomyces pombe*. EMBO J. **20:** 1259–1270.

Toyoshima-Morimoto, F., E. Taniguchi, N. Shinya, A. Iwamatsu and E. Nishida, 2001 Polo-like kinase 1 phosphorylates cyclin B1 and targets it to the nucleus during prophase. Nature **410:** 215–220.

Communicating editor: N. A. Jenkins